A new upper Oligocene marine record from northern Sinai (Egypt) and its paleogeographic context

Jochen Kuss and Mohamed A. Boukhary

ABSTRACT

The upper Oligocene Wadi Arish Formation is composed of a carbonate-dominated succession at Gebel Risan Aneiza (Sinai). The 77-m-thick unit disconformably overlies Jurassic to lower Cretaceous carbonates and is subdivided into three members, comprising six lithofacies units. The lower Wadi Arish member contains three units, a gypsiferous sandstone unit (Oa), overlain by two limestone units (Ob and Oc). The middle Wadi Arish member is represented by a conspicuous marl unit (Od) that is overlain by two upper limestone units (Oe and Of) of the upper Wadi Arish member. We discuss the euphotic subtidal depositional environments in conjunction with macro- and microfacies characteristics. Six microfacies types are defined, dominated by grain associations of rhodoliths, larger benthic foraminifera (rotaliids), corallinaceans, bivalves, peloids, few corals, and bryozoans. They characterize rhodalgal associations, common in non-tropical warm-temperate settings. Biostratigraphy is based on larger foraminifera. The middle Wadi Arish member corresponds with SB 23 (Chattian) and may correlate with Pg50, a regional maximum flooding surface. Our sequence stratigraphic interpretations define a late lowstand to early transgressive systems tract (lower Wadi Arish member), a late transgressive systems tract (middle Wadi Arish member), while the upper Wadi Arish member reflects highstand conditions. The paleogeographic setting and sequence stratigraphic interpretation of this unique upper Oligocene outcrop is placed in context of the northeast African-Arabian region.

INTRODUCTION

In comparison to the widespread distribution of Paleocene to Eocene rocks in the Levant and the Middle East, Oligocene strata are recorded from only a few outcrops of restricted extent. Within the Mediterranean coast and the Red Sea/Gulf of Suez regions Oligocene exposures are patchy in occurrence. This is due to erosion, as a consequence of tectonically induced uplift, enhanced by a major mid-Oligocene global sea-level fall (Haq et al., 1988; Haq and Al-Qahtani, 2005). The important factors controlling uplift of the Arabian Plate during the late Eocene-early Miocene interval was summarized by Schattner et al. (2006). Among them, ongoing collision of the Arabian-African and Eurasian plates, the Afar mantle plume and the initiation of rifting (and updoming) of the Red Sea, and thermal relaxation of the Arabian Plate are of major importance within the area under consideration (Figure 1).

The few Oligocene sediments exposed in Egypt are mainly represented by continental to fluviatile or deltaic siliciclastics, described, for example, from the Fayum area (Bown and Kraus, 1987). Only in the subsurface of northern Egypt (including north Sinai) have marine siliciclastics and marly limestones of Oligocene age been revealed in several wells (Soliman and Orabi, 2000; El Heiny and Enani, 1996; Ouda, 1998). These units reach thicknesses of several 100 m and evidence a down-warped Oligocene succession that is buried under younger strata. The interfingering of prodeltaic sediments with open-marine basinal deposits are documented from more distal modern-day offshore areas (Dolson et al., 2002).

The shallow-marine strata of Risan Aneiza described here represent a unique suite of Chattian (upper Oligocene) carbonates and allow the detailed study of their litho- and biofacies. The Oligocene sections are exposed in isolated outcrops, overlying Jurassic or karstified Lower Cretaceous units (Figure 2). Detailed mapping of the Oligocene strata indicates a regional dip of 10° to 15° towards southeast coinciding with onlap patterns towards the west. Six columnar sections were measured at the eastern scarp of the Risan Aneiza along a NE-trending transect. They demonstrate variations
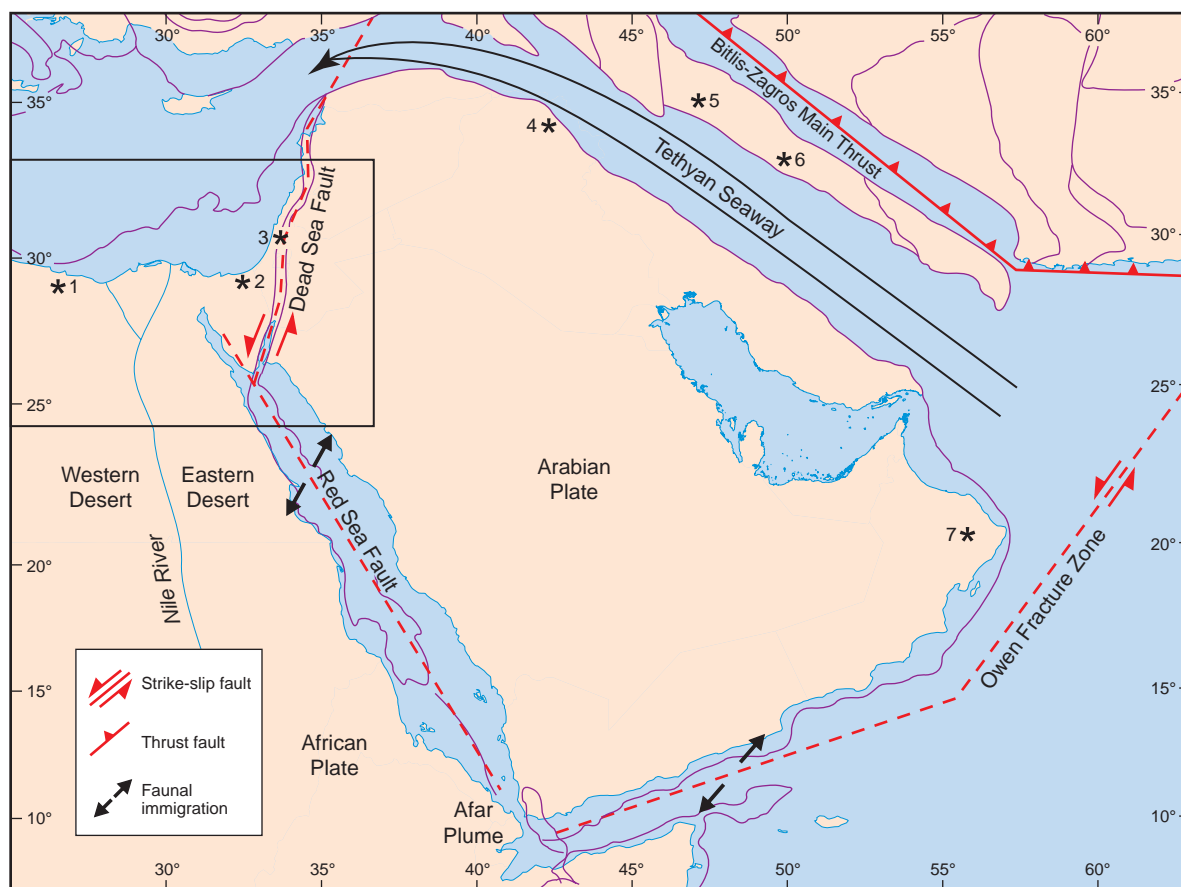
Figure 1: The major tectonic elements affecting the Arabian Plate during Oligocene-Early Miocene times. (Plate-tectonic basemap at 28.4 My – base Chattian (purple lines indicate former coastlines) from: http://www.odsn.de/odsn/services/paleomap/paleomap.html). Blue lines are present coastlines. Arrow indicates "faunal immigration" (after Rögl, 1998). Asterisks indicate descriptions of Chattian shallow-water limestones with larger foraminifera: (1) Ouda (1998), (2) own description, (3) Buchbinder et al. (2005), (4) van Bellen (1956)-revised by Sharland et al. (2004), (5) James and Wynd (1965), (6) Amir-Shahkarami et al. (2007), and (7) Jones and Racey (1994).

in lithology, total thickness and bed thickness, as well as biogenic content, and carbonate facies. The succession has been subdivided into six lithofacies units (Oa–Of, see Figure 3). The quarried area of sections I to III (Figure 2) gave the best insights into the lithostratigraphic units Ob–Of.

The Risan Aneiza Mountains (20 km south of El Arish, Figure 2) represent the northernmost outcrop of Mesozoic rocks in the Sinai Peninsula. There are few geological studies in the area, probably due to the thick sand cover over most of the mountains. Only a few studies dealing with the Cretaceous biofacies and stratigraphy of Northern Sinai included relevant data from this area (Hume, 1962; Bachmann and Kuss, 1998; Bassiouni, 2002; Bachmann et al., 2003). In the Risan Aneiza Mountains at least 130 m of Upper Jurassic (Oxfordian) carbonates of the Massajid Formation are exposed in the north, and a 280-m-thick Lower Cretaceous (Aptian – early Albian) succession of limestones intercalated with sandstones and pelites (Risan Aneiza Formation) is exposed in the central parts. Massive limestones and dolomites of middle Albian to Cenomanian age (including the Halal Formation) reach 330 m in thickness and occur mainly in the southern flanks.

GEOLOGICAL SETTING AND REGIONAL STRATIGRAPHY

Central and northern Sinai is a complex block-faulted structure characterized by several ENE- to NE-trending parallel fold belts, each 15–20 km wide and bounded by deep-seated normal faults. Its northernmost rim is down-warped towards the Mediterranean Basin along a hinge line that lies only a few kilometers north of the Risan Aneiza. The ENE-trending asymmetric domal anticlines (Figure 2)
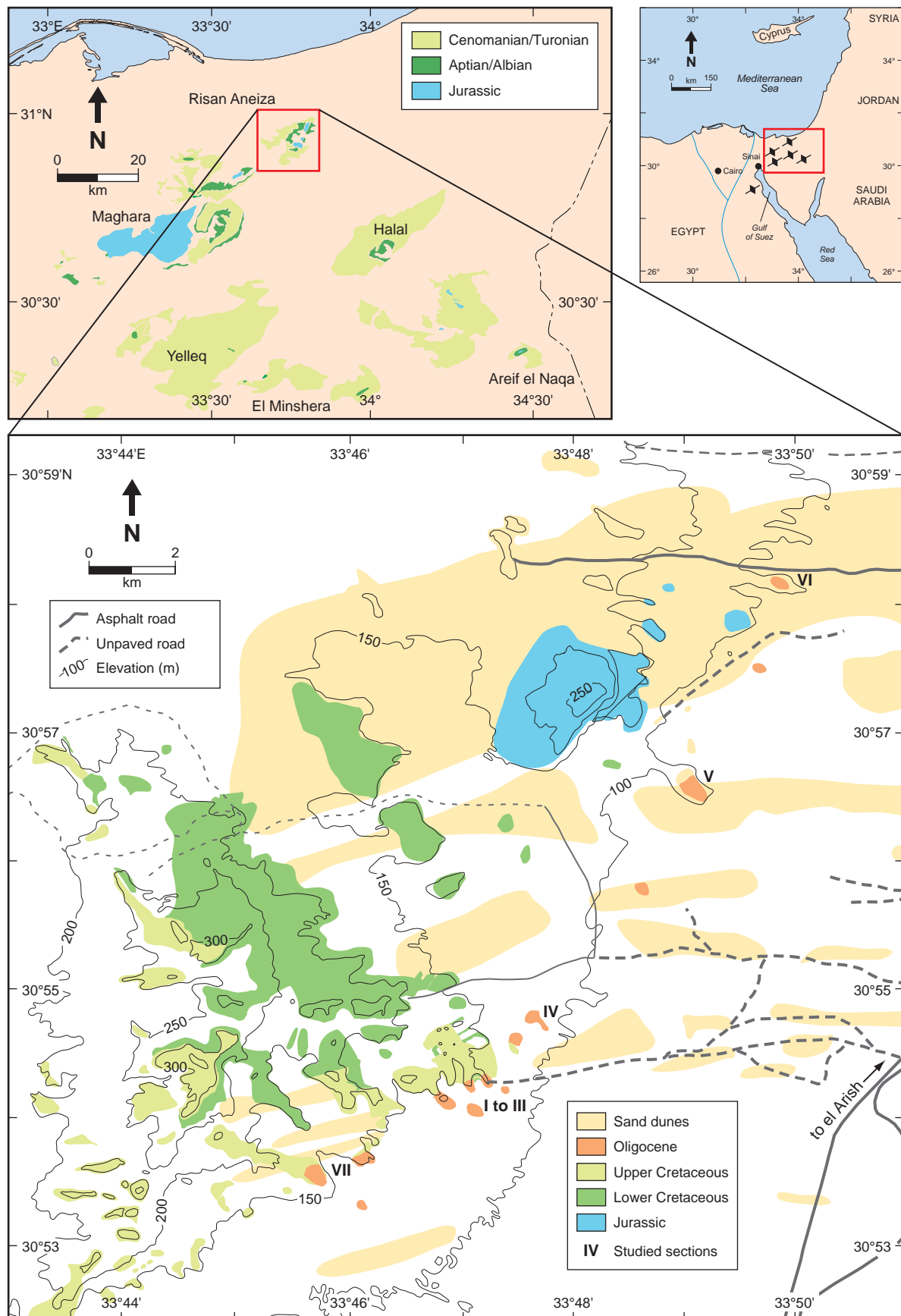
Figure 2: Geological map of the Risan Aneiza Mountains (modified after Krieter et al., 2003) with position of the upper Oligocene sections (I to VII) at the eastern flank. The geographic position is indicated in the inlay-maps.

of the Syrian Arch System (Krenkel, 1924) are exposed along the northeastern margin of the African and Arabian plates and contrast with the tectonically less-deformed intraplate settings further south. Most anticlines of the Sinai Peninsula are deeply eroded and exhibit structural similarities manifested in steep southeastern flanks (dipping up to 90°, locally overturned) and gently dipping (10–15°) northwestern flanks.

The southern to southeastern flanks may be underlain by reverse faults as indicated by repetitions of the stratigraphic units recorded at outcrops and in the subsurface (Ayyad and Darwish, 1996). The eastern scarp of the Risan Aneiza is marked by a NE-trending zone of several en-echelon fold structures within the Albian-Cenomanian succession, which are interpreted as a result of right lateral transtension along a major fault. This zone runs more-or-less parallel with the disconformable contact of the Oligocene strata against older units, suggesting an onlapping contact towards a pre-Oligocene relief that was also confirmed by westward thinning Oligocene sediments. Uplift movements of the Risan Aneiza persisted in post-Oligocene times as indicated by later erosion of Oligocene and younger sediments. To which extent the Oligocene sea had probably covered other domal structures in north Sinai (e.g. Gebel Maghara, Gebel Halal) remains to be demonstrated in future studies.

A new geologic map (scale 1:20,000) of the Risan Aneiza has recently been compiled by Krieter et al. (2003) (Figure 2), and formed the basis for this study. The measured Oligocene sections were represented by a unique limestone-marl-succession, up to 77 m thick.

In the *Eastern Desert* of Egypt (Quseir area), the Oligocene Nakhul Formation (El Akkad and Dardir, 1966) is composed of 60 m of coarse breccia and large angular limestone and chert concretions derived from the underlying Thebes Formation. Further north, between Gebel Ataqa and North Galala, Sadek (1926) reported several Oligocene coarse and "false-bedded" sandstones with bands of rounded flint and quartz pebbles. The Oligocene Gebel Ahmar Formation (Barron, 1907; Shukri, 1954) is 40–100 m thick and varicolored, composed of friable and bedded coarse-grained sandstones including silicified dark brown fossil tree-trunks.

In the *Western Desert* of Egypt, the lower Oligocene Gebel Qatrani Formation (Beadnell, 1905) is composed of up to 340 m sandstones, sandy mudstones, and minor carbonates (3%) that yielded mollusca including *Lunna, Arca, Mutela, Unio, Turritella* (Beadnell, 1905, p. 58). Also, the section is very rich in vertebrate fauna: Simons (1959, 1967, 1972) identified numerous remains of land animals, crocodiles, tortoises and turtles, besides huge quantities of silicified wood. Depositional conditions are interpreted as estuarine to fluvio-marine. Dolson et al. (2002) summarized the existing knowledge of the biota and small-scale facies variations of the famous vertebrate findings.

The Oligocene subsurface succession of the areas northward of the Western Desert consists of fine-grained siliciclastics with few intercalated carbonates. The latter contain larger foraminifera (Hassan et al., 1984; Ouda, 1998) comparable to those from Libya (Imam and Galmed, 2000) as well as to those from the Risan Aneiza. The circum-Arabian distribution of some selected upper Oligocene shallow-water limestones with larger foraminifera is indicated in Figure 1.

METHODS

The basis of this study was a microfacies analysis of 47 thin sections (cut perpendicular to the bedding plane) of 8 x 10 cm size. A semi-quantitative component analysis was conducted comprising descriptions of textural (including sorting and roundness of the components) and diagenetic features. For limestone classification we used the schemes of Dunham (1962) and Embry and Klovan (1972) with the following abbreviations: ms, mudstones; ws, wackestones; fs, floatstones; rs, rudstones; ps, packstones; gs, grainstones. Typical components and/or important textural features are used additionally to express the relative quantity of other important components (e.g. rhodolith ps).

Four marly-shale samples were used for washing and micropaleontologic studies; 37 additional thin sections were made from isolated larger foraminifera and rhodoliths. Systematic determinations of foraminifera mainly follow descriptions of Loeblich and Tappan (1988), Heck and Drooger (1984), Drooger and Magne (1959), Eames et al. (1962), Eames et al. (1968), Ellis and Messina (1965), and

Banner and Hodgkinson (1991), determinations of red algae follow descriptions of Bassi (1998), Bosence (1991), Braga et al. (1993), Braga and Aguirre (1995), and Rasser and Piller (1999).

Digital photographs of thin sections were taken with an Olympus DP 15 camera mounted on a Vanox microscope. The thin sections were deposited at the Geochronology Group of the University of Bremen (Germany) and at the Stratigraphy Group of Ain Shams University Cairo (Egypt).

BIOSTRATIGRAPHY AND LITHOSTRATIGRAPHY

The biozonation of the Oligocene section of Risan Aneiza was based on larger foraminifera. Several samples were examined for nanoplankton content, but all were barren (Marzouk, personal communication, 2007). Biostratigraphic data provided by earlier authors for the marine Oligocene sediments of Egypt were taken into consideration (Hassan et al., 1984; Cherif et al., 1993) and compared with more regional schemes (Cahuzac and Poignant, 1997; Sharland et al., 2004).

Among the identified larger foraminifera *Miogypsinoides complanatus* (Schlumberger, 1900) represented a marker species. The vertical distribution of the larger foraminifera and corallinaceans is illustrated in Figure 6. Following the biozonation concept proposed by Cahuzac and Poignant (1997) for shallow-water Oligocene deposits of western European basins, *M. complanatus* indicates SB 23 (SB = shallow-water benthic) – a late Oligocene, Chattian age (24.5 Ma, Gradstein et al., 2004) (Figure 5). This is confirmed by Vaziri-Moghaddam et al. (2006) and Amirshahkarami et al. (2007) who re-evaluated the biostratigraphy of the *Miogypsinoides*-bearing limestones of the lowermost Asmari Formation (Zagros Mountains, Iran) and concluded a late Oligocene age. According to Sharland et al. (2004) *M. complanatus* is the most indicative species of the late Oligocene (Chattian) in the Middle East. The authors redefined the circum-Arabian maximum flooding surfaces (MFS) of the late Paleogene (Sharland et al., 2001) and compared clean carbonates with *M. complanatus* of the Zagros Mountains range (Adams and Bourgeois, 1967) and in northern Iraq (van Bellen, 1956) with a new maximum flooding surface (MFS) Pg50 of Chattian age.

Most of the marine Oligocene lithostratigraphic units of Egypt were based on the names for formations and members that were established by geologists working for oil companies for subsurface fine-grained siliciclastics (e.g. El Heiny and Enani, 1996). The outcrops are restricted to coarse-grained continental deposits only (Beadnell, 1905; Barron, 1907; Shukri, 1954; Bown and Kraus, 1987). The newly discovered late Oligocene succession of Risan Aneiza, however, differs lithologically from other outcrops in Egypt and therefore justifies the introduction of a new formation.

Wadi Arish Formation

The Wadi Arish Formation was named after Wadi Arish, a large wadi that drains the Central Sinai Peninsula in the south and discharged in the Mediterranean Sea to the east of El Arish town. The type section IV at Risan Aneiza (Figures 2 and 3) is composed of limestones and clayey marls of late Oligocene age and was measured on the eastern flanks of the Risan Aneiza (Figure 2). The formation was divided into the following three members from base to top.

Lower Wadi Arish Member (comprising lithofacies units Oa to Oc – Figure 3). This member is best exposed in section IV at the eastern flanks of Risan Aneiza (Figures 2 and 3), where it unconformably rests on karstified Albian limestones of the Risan Aneiza Formation. In the type section, the lower Wadi Arish member measures about 42 m in thickness (including a gap of 10 m between units Oa and Ob). Coarse-grained sandstones intercalated with gypsum layers characterize the lowermost lithofacies Oa. Above this, massive limestones of Ob with larger foraminifera and corallinacean algae follow. Lithofacies Oc is composed of well-bedded limestones with cyclic stacking patterns. Larger foraminifera and corallinacean algae were again frequent constituents.

Middle Wadi Arish Member (comprising lithofacies unit Od – Figure 3). This member (equivalent to lithofacies unit Od) is composed of grayish-bluish clayey marls with thin intercalated layers of nodular limestones or rhodoliths. It measures up to 8 m in thickness and is characterized by sharp
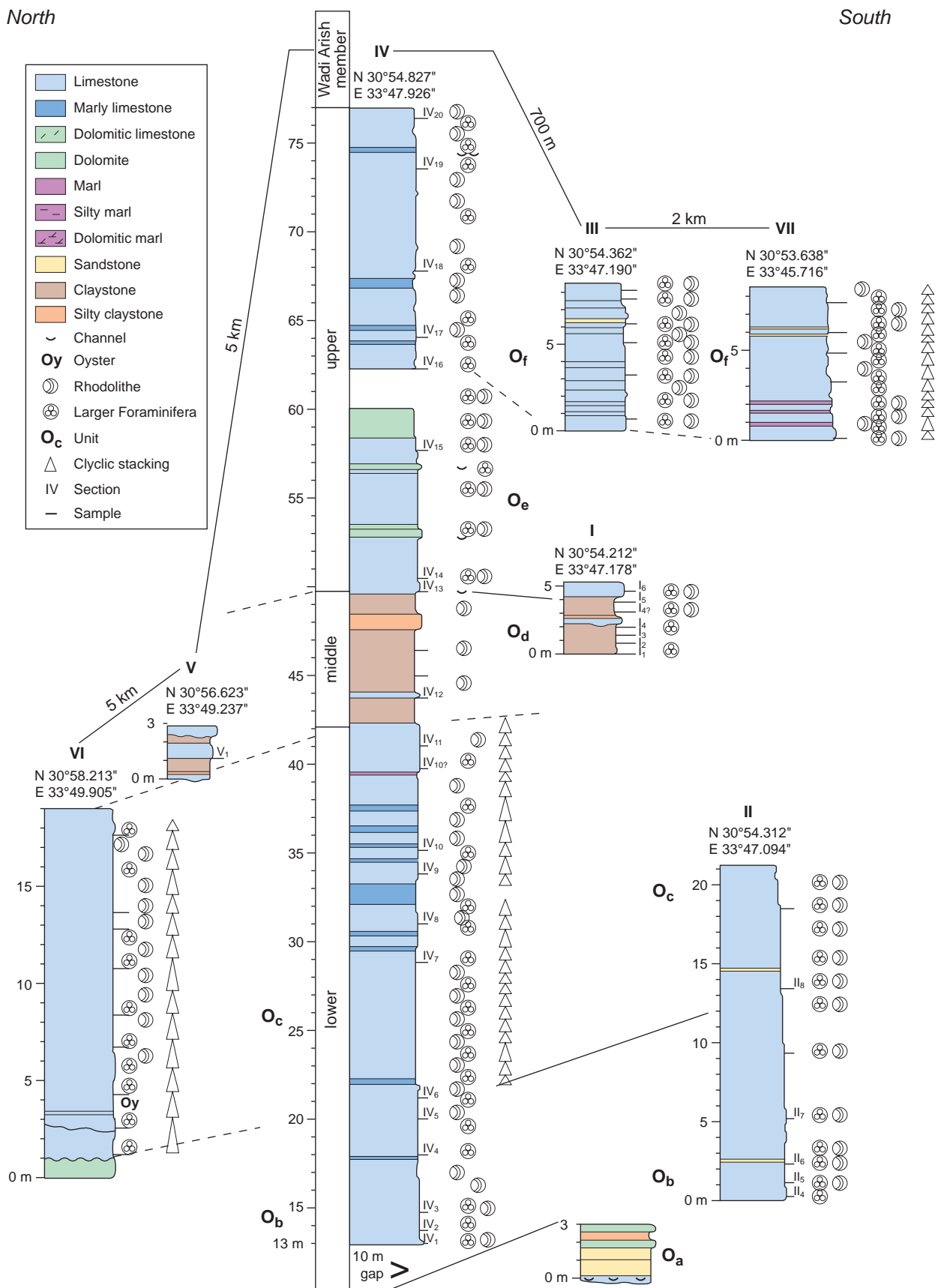
Figure 3: Lithostratigraphic correlation of four Upper Oligocene sections at the Risan Aneiza along a NNE-trending transect (see Figure 2). The boundaries between units O$_a$ to O$_f$ are marked with solid lines (certain boundaries) or dashed lines (uncertain boundaries).
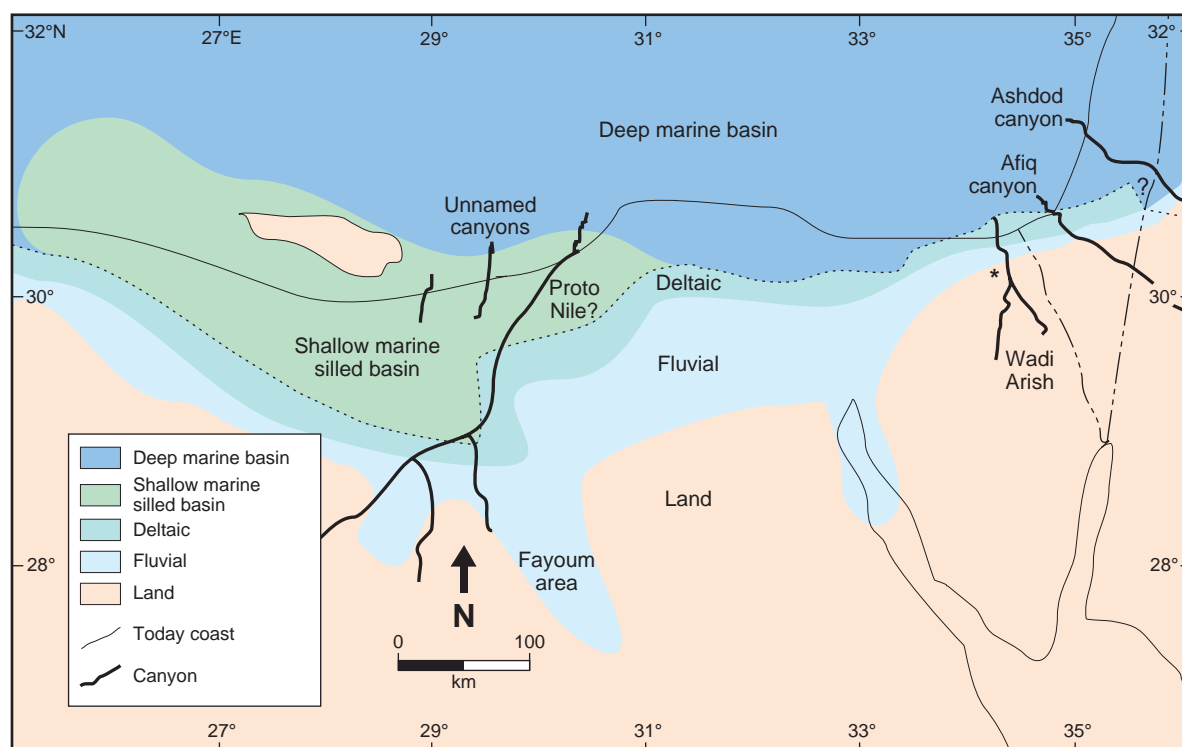
Figure 4: Paleogeography of the late Rupelian strata along the northern rim of the Arabian-African plates, summarized after various data: Rögl (1998), Meulenkamp and Sissingh (2003), Dolson et al. (2002), Sheikh (1990), Ouda (1998), El-Heiny and Enani (1996), Soliman and Orabi (2000), Issawi and McCauley (1993), Buchbinder et al. (2005). The major Oligocene to Miocene fluvial incisions are highlighted by canyon-drainages. Further paleo-rivers ("Gilf River", "Tarfa River" and "Qena drainage system" - Issawi and McCauley, 1993) are not indicated. The position of the described Chattian limestone are indicated by the asterisk West of Wadi Arish.
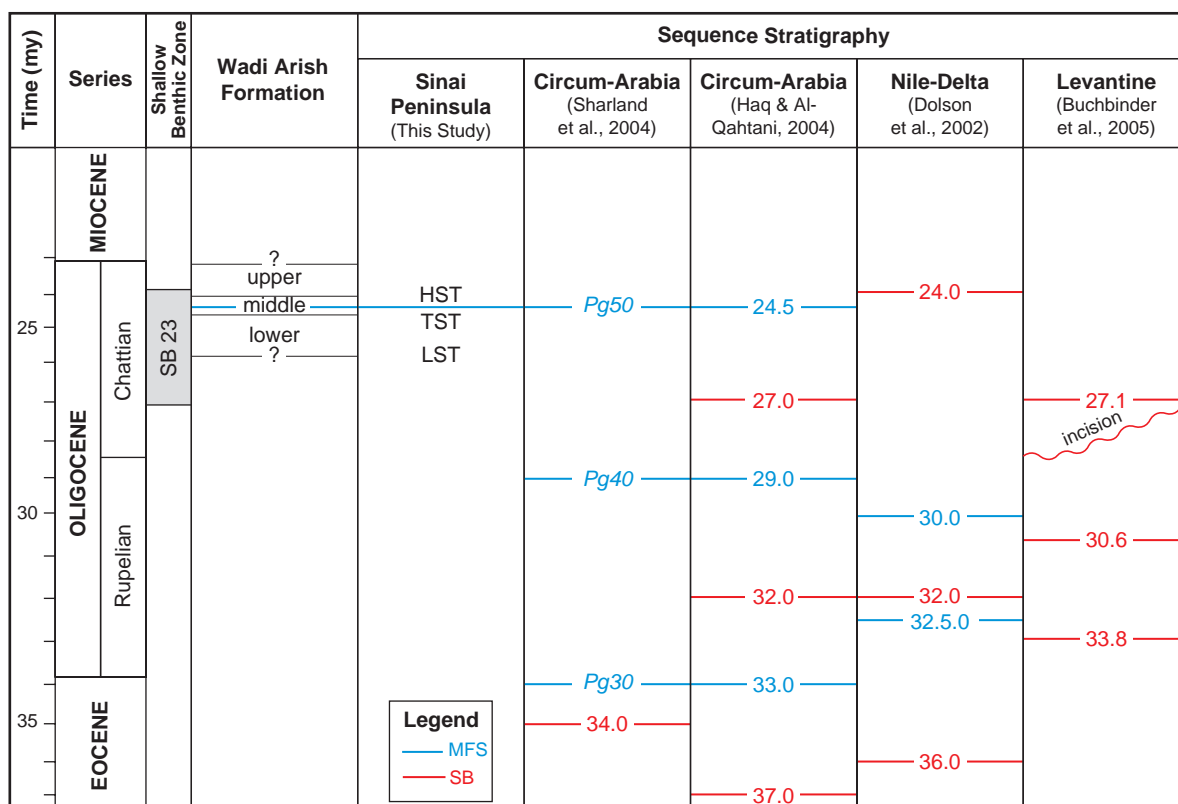
Figure 5: Sequence stratigraphic interpretations boundaries of the Wadi Arish Formation in comparison with data from various authors of the region. Timescale after Gradstein et al. (2004) with SB 23 (after Cahuzac and Poignant, 1997).

Member (Wadi Arish Formation)	Lithofacies unit	Larger Foraminifera								Corallinacean Algae				
		Amphistegina sp.	*Globotextularia* sp.	*Eulepidina elephantina*	*Heterostegina (V). assilinoides*	*Miogypsinoides complanatus*	*Nephrolepidina* gr. *morgani*	*Nephrolepidina* sp.	*Risananeiza nodosa* n. gen. n. sp.	*Lithothamnium* cf. *ramonissimum*	*Lithothamnium* sp.	*Lithoporella melobesoides*	*Neogoniolithon* sp.	*Sporolithon* sp.
Upper	O_f							■				┊	■	
	O_e							■			■		■	■
Middle	O_d	■	■	■	■	■	■	■	■		■		┊	┊
	O_c	┊	┊								■		┊	┊
Lower	O_b	■								■	■		■	■
	O_a													

Figure 6: Stratigraphic distribution of important biotic components determined on generic or species level within the six lithofacies units of Wadi Arish Formation.

contacts to carbonate lithologies below and above. This member occurs in the type section IV as well as in section III and in further outcrops along the eastern flanks of Risan Aneiza.

Upper Wadi Arish Member (comprising lithofacies units Oe to Of – Figure 3). This member is composed of pure limestone lithologies, either massive or well bedded. The latter denotes cyclic stacking patterns in the upper parts of the member similar to those of the lower Wadi Arish member. Larger foraminifera as well as algal rhodoliths are common in the 26.5 m thick Upper Wadi Arish member.

RESULTS

Description of Lateral and Vertical Macroscopic Features

Lithostratigraphically, the marine late Oligocene sediments of the Risan Aneiza are formed by two carbonate units, separated by a clayey marl unit. The most complete marine Oligocene succession has been measured at section IV (Figure 3) and has been subdivided into five carbonate and clayey marl lithofacies units (Ob–Of), underlain by the sand unit Oa.

Unit Oa: Brown sandstones and platy gypsum beds of the lowermost lithofacies unit Oa underly the carbonate dominated succession (Ob to Of) and disconformably overly middle Albian carbonates along a karstified surface (Figures 7 and 8). A 10-m-thick gap between the Oa and the lowermost limestones of Ob is assumed to be composed of siliciclastics and/or evaporites. In the quarry section II lithofacies unit Ob disconformably overlies Late Albian limestones, without lithofacies Oa between (Figure 9). Here, the disconformable boundary between Albian and Oligocene carbonates of unit Ob is not easily discernable, because of lithologic similarities. Moreover, the identification in the field between the gray micritic Albian limestones and the coarse-grained oncolithic Oligocene limestones is hampered by later diagenetic overprinting that affected and masked both units. In a few outcrops of the quarried area, bedding-parallel silicification occurs in the uppermost parts of the massive Albian carbonates several dm below the disconformity surface (Figure 10). This may be due to pre-late Oligocene diagenetic alterations possibly caused by downward-directed fluids that percolated the Albian limestones during a terrestrial interval.

Figure 7: Late Oligocene strata at the eastern flank of the Risan Aneiza with onlapping patterns against Albian carbonates of section V (see text and Figure 2).

Figure 8: Disconformity between Albian carbonates and Oligocene sandstones and evaporites of unit O_a close to section V (see text and Figure 2). Note the irregular karstified surface between both units (stippled line).

Figure 9: Disconformity between Albian carbonates and upper Oligocene limestones of the lower Wadi Arish member (lithofacies unit O$_b$) in the quarry of section II (see text and Figure 2). Lithologically, the boundary is hard to define because of similar carbonate lithologies above and below the disconformity. Vertical cleavage is due to blasting (person as scale).

Figure 10: Silicification within chalky limestones of the topmost Albian in the quarry (near section III, text and Figure 2), indicating a close position to the Albian-Oligocene disconformity.

Unit Ob: This unit reaches 10 m in thickness and is composed of massive packstones mostly several decameters thick, only a few reach 1.0 m in thickness. The matrix is composed of larger foraminifera; a few planktic foraminifera and smaller benthic foraminifera were found. Moreover, red algal fragments and extraclasts occur together with conspicuous rhodoliths of up to 12 cm in diameter. Siliciclastic components (mainly quartz grains) may reach up to 10% with slowly decreasing values in the unit above.

Unit Oc: This unit follows above and is approximately 22 m thick and composed of cyclically bedded marl-limestone couplets, each with a thickness of 0.5 to 1.3 m (Figure 11). The base of an ideal cycle consists of marly limestones (A), overlain by packstones with larger foraminifers (B) and rhodolithic rudstones (A). Twenty-five cycles were measured, but several are only represented by rhodolithic rudstones (A). Few oysters and driftwood fragments are present in (A). Whether or not orbital-forcing directly or indirectly controlled the cyclicity of the unit Oc sediments is beyond the scope of this contribution.

Unit Od: Unit Oc passes with a sharp boundary into Unit Od above, which is composed of grayish-bluish clayey marls, up to 8 m thick (Figure 12). The exact thickness of unit Od remains unclear because of sliding and deformation from later tectonic displacements. This pelitic unit can be found in several outcrops where it contains layers with rhodoliths as well as horizons with larger foraminifera. It was subdivided in two (micropaleontologically defined) sub-units: the lower is characterized by *Eulepidina elphantina* (Figure 6).

Unit Oe: follows above and has a total thickness of 10 m. It is composed of massive limestone beds, mainly packstones and grainstones, each up to 1.0 m in thickness. The proportion of siliciclastic components is less than 5%. A sharp erosive contact formed by scoured channels is obvious at the lower boundary of this unit with Od (Figure 13) as well as within Oe itself. The sandy matrixes of both limestone types are composed of larger foraminifera, smaller benthic foraminifera and biotic fragments, a few rhodoliths (locally accumulated – Figure 14) may also be found.

Figure 11: Cyclic patterns within limestone unit O$_c$ with rhodolith accumulations (A) alternating with foraminiferal packstones (B) of section III.

The topmost unit Of: This unit is 15 m thick and composed of thick-bedded and massive limestones, again with rhodoliths, biotic fragments and larger foraminifera. Cyclic stacking patterns occur in the southern section VII. The upper boundary of unit Of shows irregularities and uneven surfaces due to erosion processes.

Microfacies Description and Interpretations

Texture: Most thin sections show mud-supported textures of mudstones and wackestones (ms and ws). Among the grain-supported textures, packstones (ps) prevail over partially washed packstones and grainstones (gs). Bioturbation is locally recognized in thin sections. Borings occur in many clasts and rhodoliths; completely micritized grains and micrite envelopes are common taphonomical features.

Skeletal components: A large variety of benthic foraminifers have been identified in the studied limestones and marls, among them *Amphistegina* sp., *Nephrolepidina* gr .*morgani* (*Nephrolepidina sinaica* n. sp.), *Eulepidina elephantina*, *Risananeiza nodosa* n. gen. n. sp., *Heterostegina (Vlerkina) assilinoides*, *Globotextularia* sp. and *Miogypsinoides complanatus*. Calcareous algae are represented by a diverse corallinacean microflora: *Lithoporella melobesioides* (Plates 1.4 and 1.5), *Spongites* sp. (Plates 2.5 to 2.8), *Lithothamnium* cf. *ramosissimum* (Plates 1.1 and 1.2), *Lithothamnium* sp. (Plate 1.3), *Sporolithon* sp. (Plates 2.1 to 2.4), and *Neogoniolithon* sp. (Plate 1.6) may be present. The stratigraphic distribution of the biota was summarized in Figure 6.

Varying amounts of bivalves, gastropods, echinoderms, ostracods, bryozoans, and serpulids occur in most microfacies types. Individual representatives of these groups are not indicative of a specific depositional environment, but together with other components they represent facies-indicative assemblages. Oyster debris is rare in thin sections, but if present, disarticulated elements of cellular shell structures produced large amounts of fine-grained particles.

Figure 12: Marly unit (O$_d$) with rhodoliths overlain by limestones of unit O$_e$, section I (quarry area - text and Figure 2).

Figure 13: Detail of the erosional contact between basal unit O$_e$ with rhodoids and the marly unit O$_d$ below.

Figure 14: Accumulation of rhodoliths of unit O$_e$ of section IV (see text and Figure 2).

Non-skeletal components: Rhodoids and peloids are the most frequent constituents of all lithofacies units and of most microfacies types (including the marly unit Od). Rhodoid nuclei include quartz grains (mainly in limestones of the lower units Ob to Oc), diverse bioclasts or reworked coated grains (Plates 3.1 and 3.2). Mud-intraclasts originated from reworking of partly consolidated carbonate mud by currents, carbonate extraclasts are represented by allochthonous limestone fragments. Both occur mostly in winnowed limestones and are characterized by differing grain composition and cements when compared to those of the host-rock.

Quartz grains may reach volumetric proportions of up to 10% in limestones of units Ob to Oc, while they are less frequent in units Oe to Of. They mirror the detrital input from the hinterland while textural maturity (sorting and roundness) allow an evaluation of water energy. Further accessory non-skeletal components are phosphate and glauconite grains.

Microfacies Types and Facies Interpretation

The following six microfacies types characterize the late Oligocene limestones of Risan Aneiza and allow environmental interpretations. Detailed interpretations of the lateral and vertical distribution of facies types will only be possible after more extensive sampling of further sections within a high-resolution lithostratigraphic frame.

Quartzose, bioclastic ps with rhodoliths

Sandy, quartzose limestones occur mainly in units Ob to Oc (few also in unit Of), and contain diverse shallow-water bioclasts (bivalves, echinoderms, bryozoans) that are associated with abundant quartz grains (fine to medium grained, moderately sorted, rounded) and accessory amounts of detrital glauconite. Peloids and fragments of corallinaceans, in part transported, are common. The matrix consists mainly of sparite, although micrite-filled moulds and micrite envelopes may occur.

These limestones were deposited in a shallow, open-marine, siliciclastic nearshore realm, because of their biotic content and textures. Those of the upper unit Oe exhibit less quartz and silicilastic grains. The high textural maturity and the predominant sparite matrix indicate higher energy conditions.

Rhodolith ps

Rhodolith-ps with bed-thicknesses of 0.2 to 0.76 m contain densely packed rhodoliths in a fine-grained detrital matrix (Figure 13). This facies type was commonly found in massive packstones of unit Oe, it also occurs in Of. The largest rhodoliths are sub-ellipsoidal and sub-spheroidal in shape (flat protuberances may occur on the surface) with mean diameters from 3.5 to 11 cm (macroids, Flügel, 2004). They are the response of coralline algae to an unstable substrate (Rasser and Piller, 1999). Their nuclei are quartz grains, diverse bioclasts or reworked rhodoliths and coated grains. The internal structure of the crusts consists of loosely packed laminar corallinacean thalli with sparitic voids in between that are compared with constructional voids *sensu* Minnery et al. (1983). Moreover, the crustose framework contains bioclastic fragments including algal crusts, larger foraminifera, bryozoans (Plate 3.4) and echinoid spines.

Although living rhodoids occur in nearly all latitudes and from shallowest water depths down to more than 200 m (Flügel, 2004), they often dominate deeper-water settings. Compared to recent examples, the Oligocene rhodoliths of Sinai exhibit many similarities with those of numerous recent deeper-water environments (e.g. Adey and MacIntyre, 1970, reported 60–90 m water depth for rhodoliths off the Hawaiian Islands; Bosence, 1983, estimated 35–55 m for those from Florida; Dullo et al., 1990, described non-geniculate corallinaceans down to depths of 60–70 m). Ancient analogues of this facies were described, for example, from the Miocene of the Maltese Island (Bosence and Pedley, 1982). We therefore interpret the textural characteristics of the Oligocene rhodoliths as deeper-water indicators.

Coral-Algal fs/rs

This facies was most frequently found in thick massive limestones (0.6–1.5 m) of unit Oe, it also appears in units Ob to Od. The bioclastic content of this coarse-grained lithology is mainly composed of larger foraminifera, algal crust debris, echinoids, bryozoans and corals. The corals are of laminar
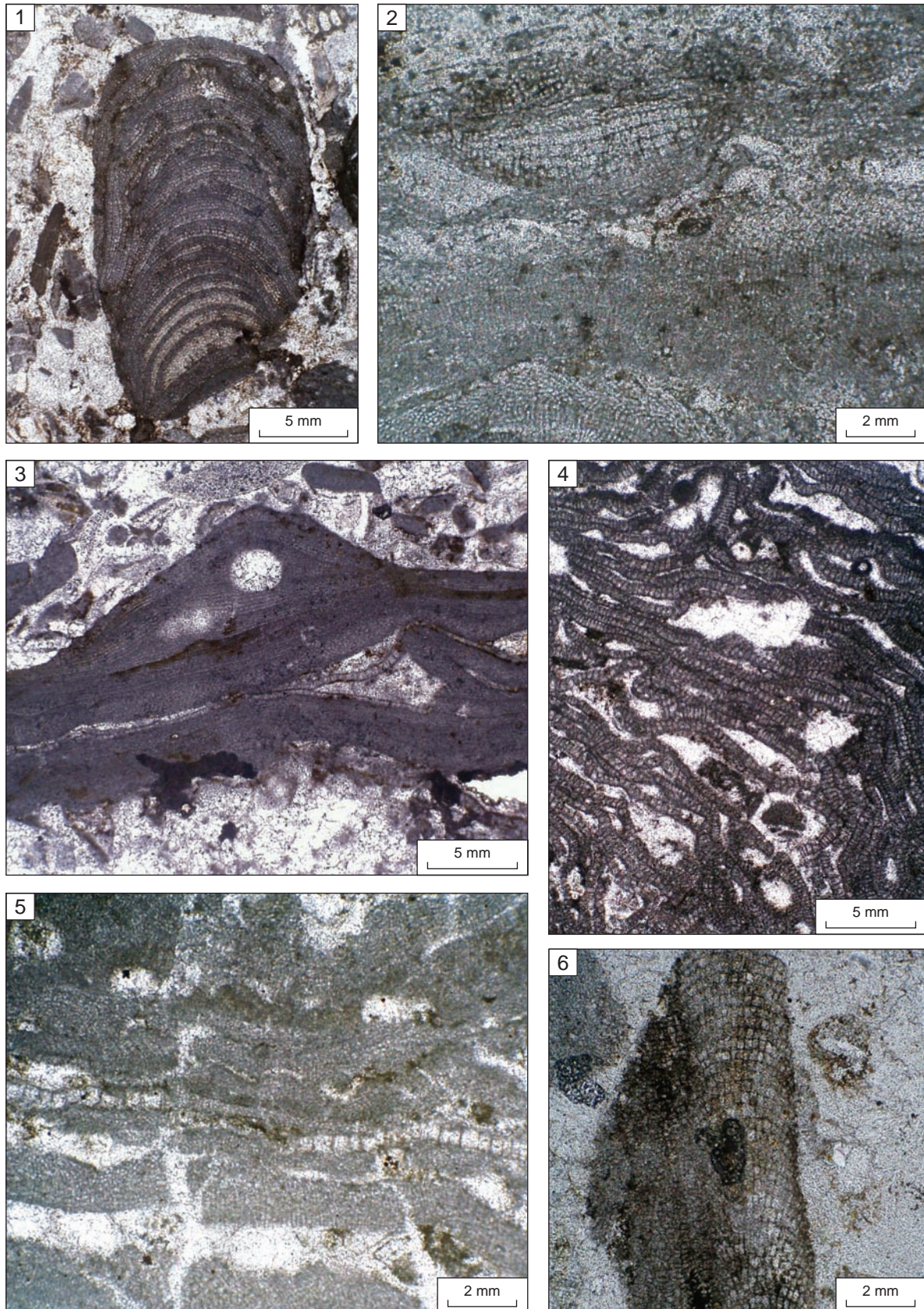
Plate 1:

(1.1) *Lithothamnium* **cf.** *ramosissimum* **(Gümbel non Reuss) Conti 1946a, branched thallus with central core of filaments diverging towards the surface of the protuberance, sample OIV/3a.**

(1.2) *Lithothamnium* **cf.** *ramosissimum* **(Gümbel non Reuss) Conti 1946a, ventral core of cell filaments, in parts "plumose hypothallus" diverging towards the substrate (arrow), sample OIV/3a.** *See facing page for continuation.*

colonies that are frequently encrusted by multiple generations of corallinaceans with bryozoans and encrusting foraminifers in between (Plate 3.5). The algal association with both geniculate and non-geniculate growth-forms is dominated by *Spongites* sp.*, Lithothamnium* sp., and *Lithoporella melobesioides*. The algal crusts may exhibit diffuse mm-scale laminations with abundant fine boundstone-crusts.

The coral fragments indicate the relative proximity to a ?reef and debris area that, along with the high muddy matrix, suggests reduced turbulence rates. The presence of coral thickets, perhaps representing biostromes or coral carpets can be envisioned for the coral-algal fs/rs facies. They can flourish in turbid, muddy environments since these corals are capable of tolerating stressful conditions by sediment shedding. However, it is important to note that there is no evidence of a complex framework or significant topography built by corals in the study area. A full interpretation of coral taxonomy, growth-form morphology and ecology is needed before a further interpretation with respect to coral paleoecology can be made.

Algal ps/rs

They form 0.2–0.5-m-thick limestones that may show cyclical repetitions with bioclastic foraminiferal grainstones of units Ob and Oe. Larger corallinacean fragments (1.5–12 mm) and larger foraminifera are the most frequent constituents of that facies; small rhodoliths, molluscs and bryozoan fragments may occur. Sorting is moderately good and bioturbation may have been extensive. This facies is transitional to bioclastic foraminiferal gs as well as to coral-algal fs/rs. The main difference between both concerns the frequency and size of corallinacean fragments and the frequency and size of rhodoliths, respectively.

The algal clasts are composed of thin free or enveloping coralline crusts and frequent small fragments of corallinaceans (Plate 3.4) with the following taxa: *Neogoniolithon* sp., *Lithothamnium* cf. *ramosissimum*, *Lithothamnium* sp. and *Spongites* sp.

These high-energy strata are formed under strong wave influence, probably also influenced by storms, as indicated by a winnowed fabric. This facies is comparable to ps/rs of platforms that have been described, for example, from Miocene carbonates of the Marion Plateau of northeastern Australia (Martin et al., 1993).
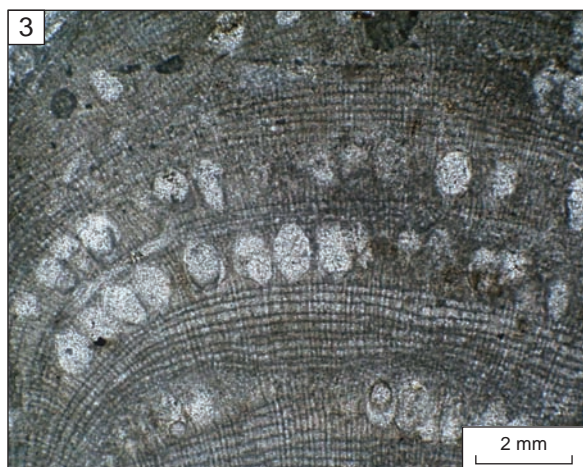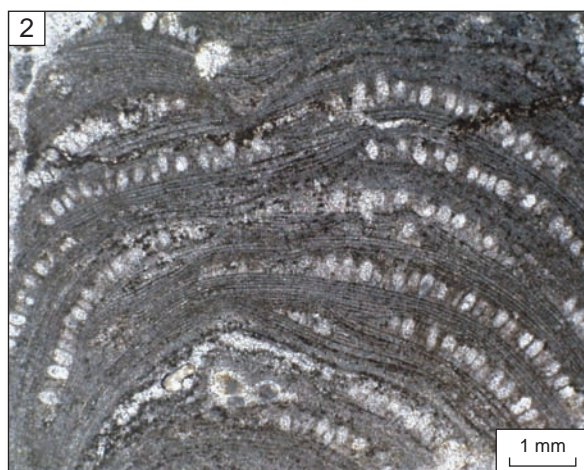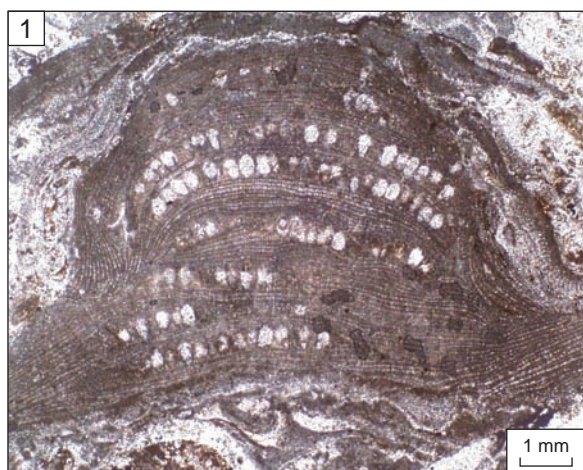
Bioclastic foraminiferal gs

The strongly bioturbated ps and gs contribute to limestones of 0.2–0.6 m thickness. This facies type is the most abundant and may occur in cyclic repetitions with algal ps/rs of units Oc and Of. The bioclastic content is mainly composed of larger foraminifera, algal crust debris, and fragments of molluscs, echinoids and bryozoans (Plate 3.6). The larger foraminifera are represented by lepidocyclinids, nummulitids and asterigerinids, while corallinacean taxa are similar to those observed in the algal floatstone facies. The quantities of these coarse bioclasts vary strongly. Bioclastic foraminiferal gs are predominantly composed of thick-walled, often rounded, rotaliid foraminifera with usually large and flat tests. The accompanying biota (erect bryozoans, echinoids and molluscs) are rarely fragmented. Non-skeletal grains are peloids and, more rarely, rounded intraclasts. Quartz, phosphates and glauconite grains are rare. Although the original textures are obliterated by strong bioturbation, cross lamination was rarely observed.

Present-day larger foraminifera with comparable test morphologies occur in the very low-energy photic zone (Haunold et al., 1997). Present-day bryozoans comparable to those of the Oligocene limestones occur anchored to the soft-bottoms in water depths down to more than 400 m (Flügel, 2004).

Plate 1 (continued):
(1.3) *Lithothamnium* **sp. and a single layer of** *L. melobesioides* **encrusting a coral (base), sample OV/1c.**
(1.4) *Lithoporella melobesioides* **(Foslie) Foslie with large palisade cells and multiple overgrowth of cell filaments, sample Ris3a.**
(1.5) *Lithoporella melobesioides* **(Foslie) Foslie (center) with multiple layers of** *Lithothamnium* **sp., sample Ris3b.**
(1.6) *Neogoniolithon* **sp. with coaxial core and peripheral filaments, sample OIV/5b.**
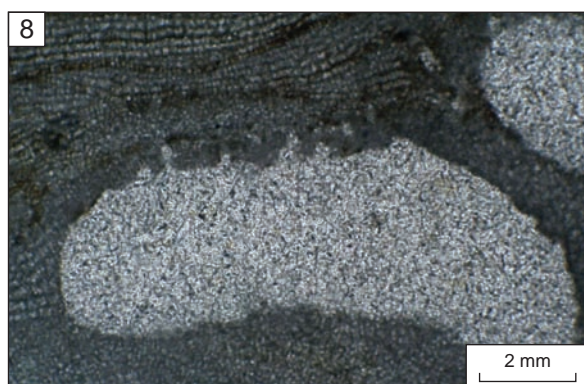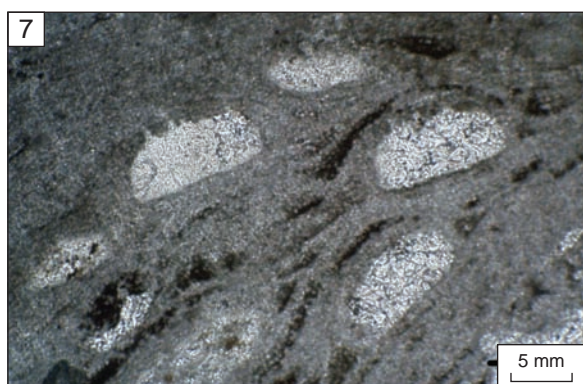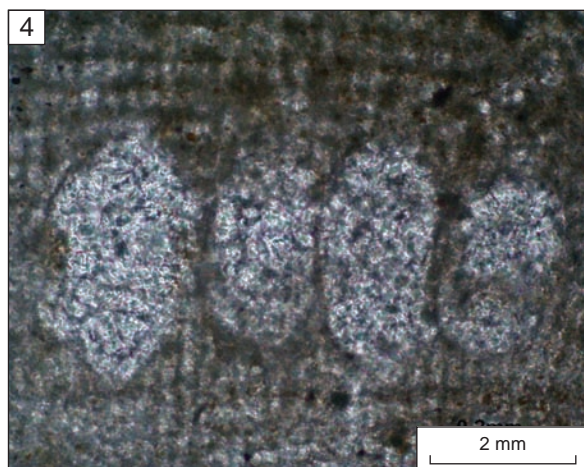
In contrast to the above-described biota, they do not depend on light. The winnowed ps rich in bioclasts and larger foraminifera are similar to algal ps/rs described above with respect to the grain composition. In the Eocene, larger foraminifera and corallinaceans were dominant, sometimes forming true bioconstructions or banks (Aigner, 1983; Taberner and Bosence, 1985). A high-energy subtidal environment of deposition is postulated, similar to storm influenced ps/rs described from recent environments by Seilacher and Aigner (1991).

Corallinacean ps with mud grains

This facies type is the most abundant in limestones of units Oc and Oe. The high-energy deposits include diverse corallinacean accumulations, dominated by debris of *Lithothamnium* sp. besides varying amounts of *Spongites* sp., both representing warm-water taxa (Flügel, 2004). Benthic foraminifera, bivalves, gastropods, echinoderms, and ostracods are also present (Plate 3.3). In addition to abundant mud peloids, well-rounded intraclastic oncoids occur. Sparry calcite is common, but wave currents possibly infiltrated mud into the pores.

Environmental constraints of modern corallines show wide latitudinal and depth ranges. Most of the warm-water corallinacean taxa prefer hard rough substrates, dim light conditions and agitated water. Intraclasts and mud peloids are formed in shallow-marine, wave- and tide-dominated regimes with continuous reworking. They are often interpreted as being formed by storm wave erosion (Flügel, 2004). Consequently, we assume high-energy-subtidal environments of deposition.

Facies Interpretation

As described here upper Oligocene limestones reflect only a small segment of a later eroded platform, and because of the limited number of available sections, we are far from detailed reconstructions of regional changes in depositional environments or of the platform architecture. However, the microfacies results allow for a discussion of the environmental aspects and a comparison of the Oligocene outcrops to similar platforms. Grain associations are essential in categorizing and interpreting microfacies types and the interpretation of the many factors that controlled their origins, including light, water temperature and salinity (Flügel, 2004). All six Oligocene microfacies types are dominated by three grain associations composed of rhodoliths, larger benthic foraminifera (rotaliinids), corallinaceans, bivalves, peloids, few corals, and bryozoans:
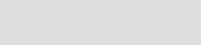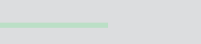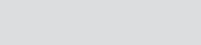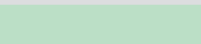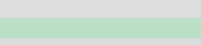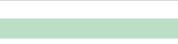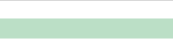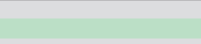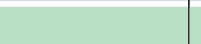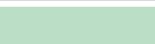
(a) Deposits of units Ob to Oe are characterized by a relatively diverse skeletal association with corals, larger benthic foraminifera, reworked corallinaceans and bryozoans. In addition, reworked clasts with planktic foraminifers may occur. Deposits of that association correspond to the algal ps/rs and to the bioclastic foraminiferal gs facies.

(b) Another frequent assemblage is characterized by prevailing corallinaceans within a foram-algal groundmass. The red algal nodules are of various sizes, always larger than 2 cm in diameter (up to 8 cm in diameter). They exhibit different types of encrustation and are mainly found in rhodolith ps. This assemblage occurs in limestones of units Od–Of.

Plate 2 (facing page):
(2.1) *Sporolithon* sp. lumpy growth with radially arranged filaments and sori of sporangial compartments, sample OIV/13a7.
(2.2) *Sporolithon* sp. lumpy growth with radially arranged filaments and sori of sporangial compartments, sample OIV/15b.
(2.3) *Sporolithon* sp. thallus section with sori of sporangial compartments; detail of Plate 2.1, sample OIV/13a7.
(2.4) *Sporolithon* sp. sporangial compartments with stalk cell at the base of a compartment, detail of Plate 2.3, sample OIV/13a7.
(2.5) *Spongites* sp. protuberance with numerous conceptacles, sample Ris6.
(2.6) *Spongites* sp. protuberance with several large conceptacles, sample OIV/13a.
(2.7) *Spongites* sp. conceptacles, detail of Plate 2.5, sample Ris6.
(2.8) *Spongites* sp. single conceptacle with multiporate roof, detail of Plate 2.6, sample OIV/13a.
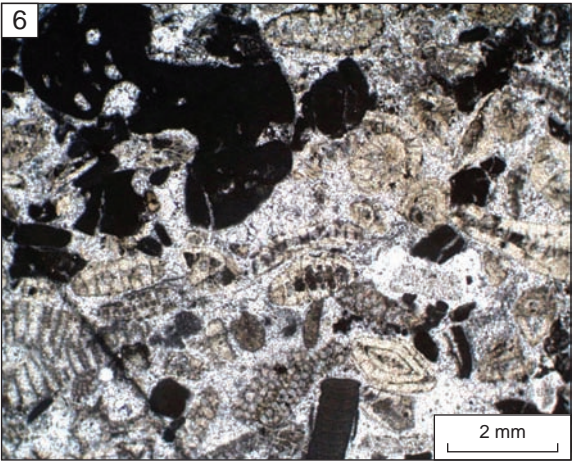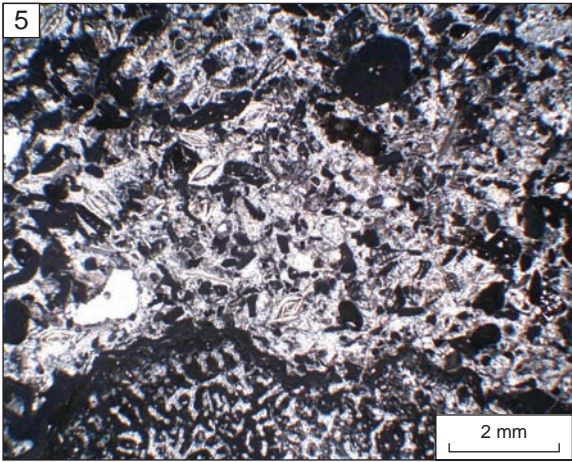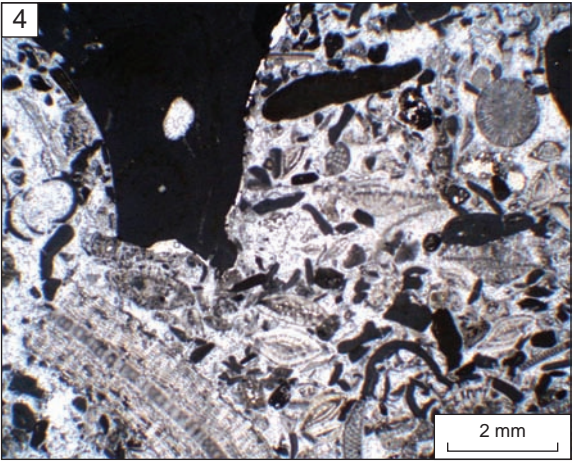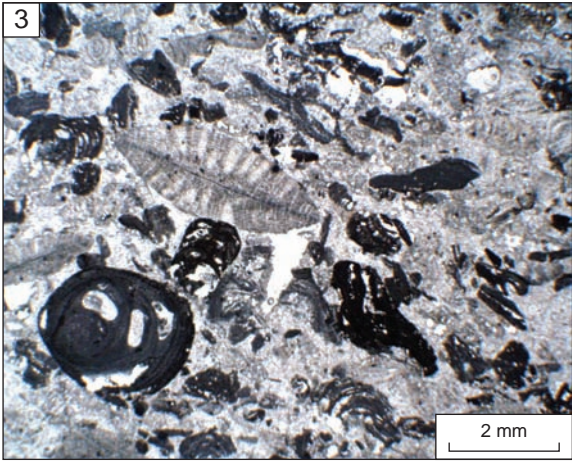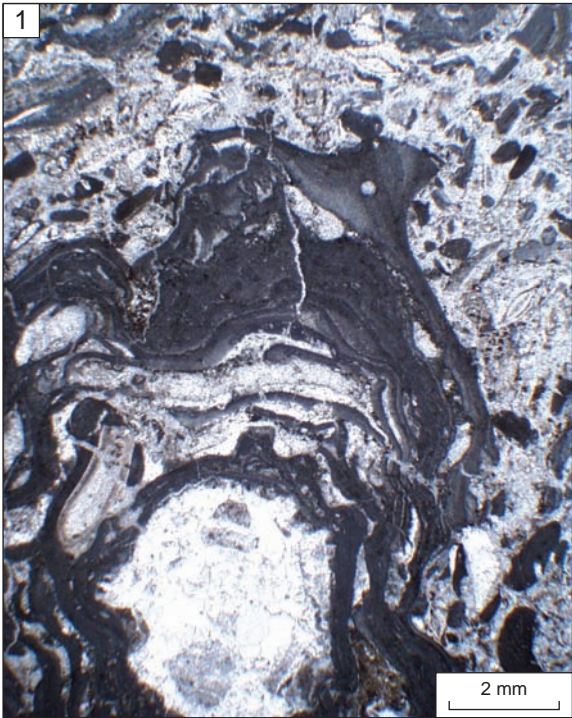
	Tropical	Subtropical	Warm-Temperature	Cold-Temperature	Cold-Water
Lees (1975)	Chlorozoan	Chloralgal			
Carannante et al. (1988)	Chlorozoan	Chloralgal	Rhodalgal		Molechlor
Ooids/aggregates					
Corals					
Green algae					
Red algae					
Foraminifera					
Bryozoans					
Molluscs					

Abundant **Common** **Rare**

Figure 15: The dominant constituents of tropical to cold-water carbonate environments (after Carannante et al., 1988; and Halfar et al., 2000). The gray area describes the Oligocene limestones of the Sinai Peninsula.

(c) Larger foraminifers with subordinate corallinaceans characterize the assemblages of algal ps/rs and bioclastic foraminiferal gs facies.

Based on the dominance of rhodoliths and larger rotaliids and the coeval absence of green algae, miliolid foraminifera, and ooids (abun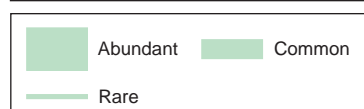dant constituents of warm-water carbonates) we placed the depositional environments of the Oligocene limestones in the "rhodalgal" zone, defined by Carannante et al. (1998) (based on Lees, 1975) for carbonates consisting predominantly of crustose red algae (> 80%, commonly rhodoids), bryozoans, benthic foraminifera, barnacles, bivalves, and echinoderms. It is transitional between chlorozoan-dominated tropical areas (with green algae, hermatypic corals) and cold-temperate ones (Figure 15). While the tropical end-member is defined by an abundance of ooids and aggregate grains, corals, and green algae, and smaller amounts of red algae, foraminifera, and bryozoans ("chlorozoan" *sensu* Lees, 1975) the warm-temperate carbonate regime is dominated by red algae, foraminifera, molluscs (including few bryozoans and corals). The boundary between the tropical zone and the warm-temperate zone (rhodalgal) is commonly drawn at the occurrence/absence of coral reefs and distribution patterns of larger foraminifera genera (Hallock, 1986; Halfar et al., 2000). We therefore classified the depositional environments of the Oligocene limestones of Sinai into a warm-temperate setting.

Carannante et al. (1998) also discussed 'anomalous' associations of environments in which the prevailing grain associations would point to a different temperature. Examples include: (1) recent subtropical hypersaline environments, possibly causing the absence of green algae, and (2) Cretaceous warm-water environments where nutrient overload caused a cold-water grain association. Compared to the studied Oligocene limestones, subtropical hypersaline conditions (1) can be excluded because

---

Plate 3 (facing page):
(3.1) Rhodoid, multi-layered corallinacean encrustations with a strongly recrystallized coral as nucleus, sample OIV/13a.
(3.2) Rhodoid, composed of corallinacean and foraminiferal encrustations, sample OIV/14a.
(3.3) Corallinacean packstone with larger foraminifers and coated grains, sample OIV/15.
(3.4) Algal packstone/rudstone with larger foraminifers and bryozoans, sample OV/1c.
(3.5) Coral-algal floatstone/packstone, sample OV/1.
(3.6) Bioclastic foraminiferal grainstone, sample RIS4.

of facies characteristics. However, high-nutrient contents (2) may have possibly triggered the depositional processes and would have promoted the growth of coralline red algae, which thrive under elevated (mesotrophic) nutrient conditions (Johansen, 1981), even though no specific nutrient data are available for the study area.

Sequence Stratigraphy

Three sequence boundaries (Dolson et al., 2002; Haq and Al-Qahtani, 2005; Buchbinder et al., 2005) and flooding surfaces (Sharland et al., 2004) were described for the Oligocene strata surrounding the Arabian Platform (Figure 5). Dolson et al. (2002) described three sequence boundaries (SB) (major unconformities) from seismic and well-log data of the Oligocene succession along the northern Egyptian coastline. Two major onlap-relations in the Rupelian and one in the Chattian (interrupted by an erosive canyon-forming event, due to the mid-Oligocene lowstand) were given by Buchbinder et al. (2005), summarizing the stratigraphy and complex depositional history of the Oligocene strata of the Levant. These two concepts showed fairly good correlations with Sharland et al. (2004) or with the "Arabian Platform Regional Sea-Level Changes" of Haq and Al-Qahtani (2005), both using the maximum flooding concept with the same nomenclature of Pg30 to Pg50 (Figure 5).

Their lowermost SB in the Oligocene overlies karstified upper Eocene (Priabonian) carbonates and is also well documented from Egypt (Ouda, 1998; Dolson et al., 2002). The age of the SB was estimated at 36 Ma (Dolson et al., 2002), 34 Ma (Sharland et al., 2004), 37 Ma (Haq and Al-Qahtani, 2005) and 34.5 Ma (Buchbinder at al., 2005) (Figure 5).

A second Oligocene SB near 31 Ma (Haq and Al-Qahtani, 2005) matches well with Buchbinder et al. (2005), while Dolson et al. (2002) determined 32 Ma.

The third Oligocene SB was placed at 27 Ma by Haq and Al-Qatahni (2005) and 27.1 Ma by Buchbinder et al. (2005), while Dolson et al. (2002) described a (?different) SB at 24 Ma. Sharland et al. (2004) defined a major flooding horizon at 24.5 Ma (Pg50) due to the presence of *Miogypsinoides complanatus* that was also evidenced in the studied sections from Sinai.

One biostratigraphically well-documented layer in the upper part of unit Od yielded *Miogypsinoides complanatus*, an index fossil of SB 23 (ranging from 24 to 27 Ma - Cahuzac and Poignant, 1997). We consequently correlated this horizon with Pg50, a regional flooding surface from circum-Arabian areas (Sharland et al., 2004) (Figures 5 and 6). Our sequence stratigraphic interpretations of the Oligocene succession includes additional facies data that defined three systems tracts; from base to top:

(a) carbonates of a (?)late lowstand to early transgressive systems tract, coinciding with units Oa to Oc,
(b) marly claystones of a late transgressive systems tract (unit Od), and
(c) carbonates of a highstand systems tract (unit Oe to Of).

(a) The sandy/gypsiferous lithologies of unit Oa (probably early lowstand deposits) are followed by carbonates of units Ob to Oc, both with remarkable siliciclastic contents. The prevailing quartzose, bioclastic ps (with rhodoliths) probably indicate a lowered base level and a closer distance to a siliciclastic dominated source area. Algal ps/rs and bioclastic foraminiferal gs of unit Ob and additional coral-algal fs/rs of unit Oc may exhibit slowly increasing water depths in carbonate dominated environments. Several intervals of both units evidence deposition in agitated water. The stacking patterns of the limestones of unit Oc are characterized by intervals of either constant, nearly equal bed thicknesses, or of upward increasing bed thicknesses. These patterns may reflect aggradational to retrogradational platform stages and therefore we interpret the carbonates of the lower Wadi Arish member (units Oa to Oc) to represent a (?)late lowstand to early transgressive systems tract.

(b) The marly claystones of unit Od are interpreted as deeper water deposits (rhodoliths etc.), sandwiched between the two carbonate units below and above. The middle Wadi Arish member was ascertained to SB 23 (see chapter biostratigraphy) and we therefore assume the marly to claystones to represent late TST-deposits that correspond with Pg50 of Sharland et al. (2004).

(c) The limestones of the upper Wadi Arish member above show reduced siliciclastic contents, high-energy (locally bioclastic) carbonates of corallinacean ps, bioclastic foraminiferal gs are often intercalated. Stacking patterns (if present) reflect upward increasing bed thicknesses that indicate retrogradational platform stages during highstand conditions. This sequence stratigraphic interpretation may be compared in future with concepts from neighboring areas.

PALEOGEOGRAPHY OF THE OLIGOCENE IN NORTHEAST AFRICA/ARABIA

The late Oligocene record of Risan Aneiza represents a marine facies which significantly revises the paleogeographic extension of the Oligocene sea over northern Egypt and the Levantine. Nowhere else in the Sinai Peninsula or northern Egypt are marine Oligocene outcrops known; marine beds of this epoch were only recorded in the subsurface (El Heiny and Enani, 1996). Further east, Avnimelech (1939) described a succession of upper Oligocene carbonates up to 50 m thick with larger foraminifera from the Judean Mountains, representing a late Oligocene marine ingression that interwedges with deltaic-fluviatile clastics of the Lakhish Formation (Hirsch, 2002). Buchbinder et al. (2005) interpreted these limestones as mass-transported boulders of the Ramla Member, indicating a redeposited carbonate platform further east.

In Egypt, the most prominent outcrops of Oligocene age are found in the Fayoum area with sandstones, siltstones and clays of the deltaic Qatrani, the fluviatile Gebel Ahmar and the lacustrine Nakheil formations (Figure 4). In his study of the El Arag area in the north Western Desert, Osman (2003) postulated that the shoreline of the Oligocene passed north of the Fayum Depression, skirting the southern flank of El Arag and continued into the Siwa Oasis, where De La Harpe (1883) gave a record of marine Oligocene. Further north, east of the Nile Delta area and in the offshore to the northwest of the Sinai Peninsula, the Oligocene (Chattian) section (including some Miocene/Aquitanian at its top) was named the Tineh Formation by El Heiny and Enani (1996). It is composed of prodeltaic sediments, interfingering with open-marine basinal deposits further offshore according to Dolson et al. (2002). The regional distribution of these facies was associated with the development of ancient river systems, which drained ancient uplifted areas in the Red Sea and Uweinat regions since early Oligocene times (Figure 4, Dolson et al. 2002; Buchbinder et al., 2005). The geographic changes and shiftings of these paleo-drainage systems during the Oligocene-Miocene interval were interpreted by Issawi and McCauley (1993). Although the exact pathways and the timing of several valleys and canyons are still under discussion (Dolson et al., 2002), their importance for long-distance transport of clastic material, for various dissection and incision processes of the shelf (especially during times of increased uplift and/or sea-level fall) is beyond question.

The ancestral Arish-valley (*sensu* Issawi and McCauley, 1993) of the northern Sinai Peninsula (Figure 4) probably flanked the upper Oligocene limestones of Risan Aneiza to the east, and thus may have demonstrated small-scale facies-variabilites within the platform. Due to the elevated position of the Risan Aneiza, the Oligocene shoreline may have been close to its eastern flanks. The marine late Oligocene strata are thus coeval with the lower part of the Tineh Formation as identified by El Heiny and Enani (1996). Equivalent deposits of the upper part of the Tineh Formation (Aquitanian) are missing in the exposed section of Risan Aneiza. This may be due to later erosion, since the thickness of the exposed section is considered residual.

Broad regional comparisons of the Oligocene of Risan Aneiza indicate stratigraphic, lithologic and biofacies similarities with the lower parts of the Asmari Limestone (a well-known Oligocene-Miocene carbonate unit of the Zagros Mountains in Iran; Slinger and Crichton, 1959; Motiei, 1993) and equivalent formations in the Kirkuk area of Iraq (van Bellen et al., 1959). Following the discussion in Sharland et al. (2004), the Pg50 MFS (maximum flooding surface) limestones (probably equivalent to the newly described late Oligocene carbonates from Risan Aneiza) yielded a circum-Arabian distribution with the following coeval occurrences (Figure 1): (1) Middle Asmari carbonates of Iran; (2) carbonates near the base of Anah Formation of Iraq; (3) middle Asmari Formation of the United Arab Emirates (Alsharhan and Nairn, 1997); (4) intra-Taqa carbonates/"Ma'hm Reef" facies of Oman (Jones and Racey, 1994); and (5) intra-Taqa Formation of Yemen (Beydoun et al., 1998).

To the west, similar lithologies have been described by Imam and Galmed (2000) from the southern Sirte Basin of Libya.

IMPLICATIONS FOR HYDROCARBON POTENTIAL

Most of the well-known commercial oil and gas discoveries in Egypt occur in the Gulf of Suez (Neogene plays) and the northern Western Desert (Mesozoic plays). The upper Paleogene to Neogene plays in the offshore Mediterranean contain significant exploration potential and will provide substantial reserve replacements in the coming decades (Dolson et al., 2000). This resource has more than doubled in the last years, largely from successful deep-water exploration for Pliocene slope-channel systems. Since late Eocene time, northern Egypt was tilted toward the Mediterranean Sea during regional uplift associated with the opening of the Gulf of Suez and Red Sea rifts. Drainage systems shed reservoir quality sediments northward in a series of forced regressions.

The Nile Delta is an emerging giant gas province with proven reserves of approximately 42 trillion cubic feet (TCF) with approximately 50 TCF yet-to-find resources (Dolson, et al., 2004). Proven reservoirs vary in age from Oligocene/early Miocene through Pleistocene. Proven source rocks include Jurassic coals and Lower Miocene shales and the condensed Qantara Formation shales (Shaaban et al., 2006). Additional source rocks may be present in condensed intervals of Cretaceous, Oligocene and Eocene age. The isolated onshore occurrence of Chattian carbonates that are described here may contribute to a better understanding of the complex depositional and erosional history during the Oligocene in Egypt.

CONCLUSIONS

The new Oligocene record of Risan Aneiza comprises a succession (up to 77 m thick) of mainly shallow-marine carbonate lithologies, restricted to a few outcrops along the easternmost flanks of the Risan Aneiza Mountains, Sinai Peninsula in Egypt. This succession was attributed to the newly defined Wadi Arish Formation, which was divided into three members. The lowermost part is exposed only directly above karstified Albian carbonates, and is represented by reddish gravelly sandstones with reworked pebbles of the underlying strata (unit Oa). These varicolored sandstones exhibit similar lithologies to other continental Oligocene strata described from various areas in Egypt. Limestones follow above (unit Ob) and are exposed also further west. They are overlain by white, hard, massive limestones with corallinaceans and larger foraminifers (unit Oc). Unit Od is formed by fossiliferous clayey marls with limestone-intercalations and overlain by two carbonate units Oe and Of, both again with corallinaceans and larger foraminifera.

Depositional architecture, thickness variation, and facies characteristics of the Oligocene sections defined along a 12-km NE-trending transect at the eastern scarp of the Risan Aneiza, indicated an eastward dipping depositional gradient against a central anticlinal core, where Upper Jurassic and Lower Cretaceous sediments crop out. Biostratigraphic analysis and sequence stratigraphic comparisons indicated a late Oligocene age (Chattian) for the middle unit Od. Sequence stratigraphic interpretations classified the lower units Oa to Oc into a late lowstand to early transgressive systems tract, the marly claystones of unit Od into a late transgressive systems tract, while the limestones of the upper units Od to Oe represent highstand conditions.

Facies and environmental interpretations of the limestones allow the following conclusions:

- They represent a platform-segment that evolved from a (?nearshore) siliciclastic environment to open shelf deposition, probably deeper water, with periods of reworking in agitated waters.
- The "rhodalgal" grain associations indicate non-tropical warm-temperate environments of deposition that are either influenced by temperature or/and by enhanced nutrient concentration. (Sea-surface temperatures below 18°C during the winter months would seriously harm coral development and would explain the virtual absence of green algae).
- Our data do not match with the "tropical incursion" of Rögl (1998) that is based on a *Lepidocyclina* horizon around the Paleogene-Neogene boundary, when Indian-Pacific

communities grew along a seaway from the Lut Block to the northwest. This warm-water transgression spread from the Middle East to the Mediterranean Sea (and to the Paratethys) and may have reached the Levant margin later.

- The large numbers of comparable circum-Arabian platform carbonates of late Oligocene age argue that the isolated occurrence of North Sinai reflects part of an extended platform system that was eroded later.

ACKNOWLEDGEMENTS

REFERENCES

Adams, C.G. and E. Bourgeois 1967. Asmari biostratigraphy. Geological and Exploration Division, Iranian Oil Offshore Company Report 1074, Unpublished.

Adey, W.H. and L.G. MacIntyre 1970. Crustose coralline algae: a re-evaluation in the geological sciences. Geological Society of America Bulletin, v. 84, p. 883-903.

Aigner, T. 1983. Biofabrics as dynamic indicators in nummulite accumulations. Journal of Sedimentary Petrology, v. 55, no. 1, p. 131-134.

Alsharhan, A.S. and A.E.M. Nairn 1997. Sedimentary basins and petroleum geology of the Middle East. Elsevier, 811 p.

Amir-Shahkarami, M., H. Vaziri-Moghaddam and A. Taheri 2007. Sedimentary facies and sequence stratigraphy of the Asmari Formation at Chaman-Bolbol, Zagros Basin, Iran. Journal of Asian Earth Sciences, v. 29, p. 947-959.

Avnimelech, M. 1939. On the geology and morphology of the Megiddo area. Journal of the Palestinian Oriental Society, v. 19, p. 18-37.

Ayyad, M.H. and M. Darwish 1996. Syrian Arc structures: A unifying model of inverted basins and hydrocarbon occurrences in North Egypt. Egyptian General Petroleum Company Seminar, November 1996, Cairo, Egypt, p. 1-19.

Bachmann, M. and J. Kuss 1998. The Middle Cretaceous carbonate ramp of the Northern Sinai: sequence stratigraphy and facies. In, V.P. Wright and T.P. Burchette (Eds.), Carbonate Ramps. Geological Society, v. 149, p. 253-280.

Bachmann, M., M. Bassiouni and J. Kuss 2003. Timing of mid-Cretaceous carbonate platform depositional cycles, northern Sinai, Egypt. Palaeogeography, Palaeoclimatology, Palaeoecology, v. 200, p. 131-162.

Banner, F.T. and R.L. Hodgkinson 1991. A revision of the foraminiferal subfamily Heterosteginidae. Revista Espagnola de Micropaleontologia, v. 23, p. 101-140.

Barron, T. 1907. The Topography and Geology of the District between Cairo and Suez. Egyptian Survey Department, p. 1-133.

Bassi, D. 1998. Coralline Algal Facies and their palaeoenvironments in the Late Eocene of Northern Italy (Calcare de Nago, Trento). Facies, v. 39, p. 179-202.

Bassiouni, A.M. 2002. Middle Cretaceous (Aptian–Early Turonian) ostracoda from Sinai, Egypt. Neue Paläontologische Abhandlungen, v. 5, p. 1-146.

Beadnell, H.J.L. 1905. The Topography and Geology of the Fayum Province of Egypt. Survey Department, p. 1-101.

Beydoun, Z.R., M.A.L. As Saruri, H. El Nakhal, I.N. Al Ganad, R.S. Barba, A.S.O. Nani and M.H. Al Aawah 1998. Republic of Yemen. International Lexicon of Stratigraphy, v III, Asia, Fascicula 10 b2, International Union of Geological Sciences Publication, v. 34, 245p.

Bosence, D.W.J. 1983. Description and classification of rhodoliths (rhodoids, rhodolites). In, T. Peryt (Ed.), Coated Grains. Springer p. 217-224.

Bosence, D.W.J. 1991. Coralline algae: mineralization, taxonomy, and palaeoecology. In, R. Riding (Ed.), Calcareous Algae and Stromatolites. Springer-Verlag, Heidelberg, p. 98-113.

Bosence, D.W.J. and H.M. Pedley 1982. Sedimentology and palaeoecology of a Miocene coralline algal biostrome from the Maltese Islands. Palaeogeography, Palaeoclimatology, Palaeoecology, v. 38, p. 9-43.

Bown, T.M. and M.J. Kraus 1987. Geology and paleoenvironment of the Oligocene Gebel el Qatrani Formation and adjacent rocks, Fayum depression Egypt. United States Geological Survey, Professional Paper no. 1452, p. 1-60.

Braga, J.C., D.W.J. Bosence and R.S. Steneck 1993. New anatomical characters in fossil coralline algae and their taxonomic implications. Palaeontology, v. 36, p. 535-547.

Braga, J.C. and J. Aguirre 1995. Taxonomy of fossil coralline algal species: Neogene Lithophylloideae (Rhodophyta, Corallinaceae) from southern Spain. Review of Palaeobotany and Palynology, v. 86, p. 265-285.

Buchbinder, B., R. Calvo and R. Siman-Tov 2005. The Oligocene in Israel: A marine realm with intermittent denudation accompanied by mass-flow deposition. Israel Journal of Earth Sciences, v. 54, p. 63-85.

Cahuzac, B. and A. Poignant 1997. Essai de biozonation de l'Oligo-Miocène dans les bassins européens à l'aide des grands foraminifers néritiques. Bulletin de la Société Géologique de France, v. 168, no. 2, p. 155-169.

Carannante, G., M. Esteban, J.D. Miliman and L. Simone 1988. Carbonate lithofacies as paleolatitude indicators: problems and limitations. Sedimentary Geology, v. 60, p. 333-346.

Cherif, O.H., H. El-Sheikh and S. Mohamed 1993. Planktonic foraminifera and chronostratigraphy of the Oligo-Miocene in some wells in the isthmus of Suez and the North-Eastern reach of the Nile Delta, Egypt. Journal of African Earth Sciences, v. 16, no. 4, p. 499-511.

De la Harpe 1883. Monographie der in Agypten und der libyschen Wüste vorkom-menden Nummuliten. Palaeontographica (n.s.) 30, p. 155-216.

Dolson, J., A. El Barkooky, F. Wehr, P.D. Gingerich, N. Prochazka and M. Shann 2002. The Eocene and Oligocene Paleo-ecology and Paleo-geography of Whale Valley and the Fayoum Basins: Implications for Hydrocarbon Expüloration in the Nile Delta and Eco-Tourism in the Greater Fayoum Basin. Cairo 2002, AAPG/EPEX/SEG/EGS/EAGE Fieldtrip Guidebook (Nr.), p. 1-79.

Dolson, J., Boucher, P., Dodd, T. and J. Ismail 2002. Petroleum potential of an emerging giant gas province, Nile Delta and Mediterranean Sea off Egypt. Oil and Gas Journal, v. 100, no. 20, p. 32-37.

Drooger, C.W. and J. Magne 1959. Miogypsinids and planktonic foraminifera of the Algerian Oligocene and Miocene. Micropaleontology, v. 5, no. 3, p. 273-284.

Dullo, W.C., E. Moussavian and T. Brachert 1990. The foralgal crust facies of the deeper fore reefs in the Red Sea: a deep diving survey by submersible. Geobios, v. 23, no. 3, p. 261-273.

Dunham, R.J. 1962. Classification of carbonate rocks according to depositional texture. American Association of Petroleum Geologists, Memoir, v. 1, p. 108-121.

Eames, F.E., F.T. Banner, W.H. Blow, W.J. Clarke and A.H. Smout 1962. Morphology, taxonomy and stratigraphic occurrence of Lepidocylininae. Micropaleontology, v. 8, no. 3, p. 289-322.

Eames, F.E., F.T. Banner, W.H. Blow, W.J. Clarke and A.H. Smout 1968. Some larger foraminifera from the Tertiary of Central America. Paleontology, v. 11, p. 283-305.

El Akkad, S. and A.A. Dardir 1966. Geology of the Red Sea coast between Ras Shagra and Mersa Alam. Geological Survey of Egypt, v. 35, p. 1-67.

El Heiny, I. and N. Enani 1996. Regional stratigraphic interpretation pattern of Neogene sediments, northern Nile delta, Egypt. 12th Petroleum Conference, EGPC, Cairo, v. 1, p. 270-290.

El Sheik, H.A. 1990. Oligocene-Miocene boundaries in some wells in the Eastern part of the Nile Delta, Egypt. Annals of the Geological Survey of Egypt, v. 16, p. 249-253.

Ellis, B.F. and A.R. Messina 1965. Catalogue of index foraminifera. Volume 1, Lepidocyclinids and Miogygpsinides. American Museum of Natural History, Special publication, 700 p.

Embry, A.F. and J.E. Klovan 1972. Absolute water depth limits of Late Devonian paleoecological zones. Geologische Rundschau, v. 61, p. 672-686.

Flügel, E. 2004. Microfacies of Carbonate Rocks. Springer, 976 p.

Gradstein, F., J. Ogg and A. Smith 2004. A Geologic Time Scale. Cambridge University Press, 569 p.

Halfar, J., L. Godinez-Orta and J.C. Ingle 2000. Microfacies analysis of Recent carbonate environments in the southern Gulf of California, Mexico - a model for warm-temperate to subtropical carbonate formation. Palaios, v. 15, p. 323-342.

Hallock, P. and W. Schlager 1986. Nutrient excess and the demise of coral reefs and carbonate platforms. Palaios, v. 1, p. 389-398.

Haq, B.U., J. Hardenbol and P.R. Vail 1988. Mesozoic and Cenozoic chronostratigraphy and cycles of sea-level change. Society of Economic Paleontologists and Mineralogists, v. 42, p. 71-108.

Haq, B.U. and A.M. Al-Qahtani 2005. Phanerozoic cycles of sea-level change on the Arabian Platform. GeoArabia, v. 10, no. 2, p. 127-159.

Hassan, M.Y., M.A. Boukhary, G. Salloum and H. Elsheikh 1984. Biostratigraphy of the subsurface Oligocene sediments in the North Western Desert, Egypt. Qatar University Science Bulletin, v. 4, p. 235-262.

Haunold, T.G., C. Baal and W. Piller 1997. Benthic foraminiferal associations in the Northern Bay of Safaga, Red Sea, Egypt. Marine Micropaleontology, v. 29, p. 185-210.

Heck, S.E. and C.W. Drooger 1984. Primitive Lepidocycline from San Vicente de la Barquera (N. Spain). Paleontology, Proceedings B 87, p. 301-318.

Hirsch, F. 2002. The Oligocene-Pliocene of Israel. In, J.K. Hall, V.A. Krasheninikov, F. Hirsch, C. Benjamini and A. Flexer (Eds.), Geological Framework of the Levant (II): The Levantine Basin and Israel. p. 459-488.

Hume, W.F. 1962. Geology of Egypt V. III. The stratigraphical history of Egypt, part I from the close of the Precambrian episodes to the Cretaceous period. Cairo, Government Printing Offices, p. 1-712.

Imam, M.M. and M.A. Galmed 2000. Stratigraphy and microfacies of the Oligocene sequence at Gebel Bu Husah, Marada Oasis, South Sirte Basin, Libya. Facies, v. 42, p. 93-106.

Issawi, B. and J.F. McCauley 1993. The Cenozoic landscape of Egypt and its river systems. Annals Geological Survey Egypt (XIX), p. 357-384.

James, G.A. and J.G. Wynd 1965. Stratigraphic nomenclature of Iranian oil consortium agreement area. American Association of Petroleum Geologists Bulletin, v. 49, p. 2182-2245.

Johansen, H.W. 1981. Coralline Algae, A First Synthesis. CRC Press, Boca Raton, 239 p.

Jones, R.W. and A. Racey 1994. Cenozoic Stratigraphy of the Arabian Peninsula and Gulf. In, M.D Simmons (Ed.), Micropaleontology and Hydrocarbon Exploration in the Middle East. Chapman and Hall, p. 273-307.

Krenkel, E. 1924. Der Syrische Bogen. Centralblatt für Mineralogie, Geologie, Palaeontologie, Abhandlungen. v. 9, p. 274-281 and v. 10, p. 301-131.

Krieter, J., C. Meissen and C. Müller 2003. Geological Map of the Gebel Risan Aneiza, North Sinai (Egypt), Scale 1:20,000. University of Bremen, unpublished diploma thesis.

Lees, A. 1975. Possible influences of salinity and temperature on modern shelf carbonate sediments contrast. Marine Geology, v. 13, p. 67-73.

Loeblich, A.R. and H. Tappan 1988. Foraminiferal Genera and their Classification. van Nostrand Rheinold Co. Inc., New York, 970 p.

Martin, J.M., J.C. Braga, K. Konishi and C.J. Pigram 1993. A model for the development of rhodoliths on platforms influenced by storms: the Middle-Miocene carbonates of the Marion Plateau (Northeastern Australia). In, J.A. McKenzie, P.J. Davies, A. Palmer-Julson et al. (Eds.), Proceedings of the Ocean Drilling Project. Science Research, College Station, v. 133, p. 455-460.

Meulenkamp, J.E. and W. Sissingh 2003. Tertiary palaeogeography and tectonostratigraphic evolution of the northern and southern Peri-Tethys platform and the intermediate domains of the African-Eurasian convergent plate boundary zone. Palaeogeography, Palaeoclimatology, Palaeoecology, v. 196. p. 206-228

Minnery, G.A., R. Rezak and T.J. Bright 1983. Depth zonation and growth form of crustose coralline algae: Flower garden banks, Northern Gulf of Mexico. In, D.F. Toomey and M.H. Nitecki (Eds.), Paleoalgology: Contemporary Research and Application. p. 237-246.

Motiei, H. 1993. Stratigraphy of the Zagros. Treatise on the Geology of Iran, Geological Survey of Iran, p. 536.

Osman, R.A. 2003. Contribution to the stratigraphy of El Arag Depression, North Western Desert, Egypt. Sedimentology of Egypt, v. 11, p. 157-167.

Ouda, K. 1998. Mid-Late tertiary foraminiferal events and stratigraphic hiatuses in Egypt. Neues Jahrbuch Geologie Paläontologie, Abhandlungen, v. 209, no. 2, p. 145-215.

Rasser, M.W. and W.E. Piller 1999. Application of neontological taxonomic concepts to Late Eocene coralline algae (Rhodophyta) of the Austrian Molasse Zone. Journal of Micropalaeontology, v. 18, p. 67-80.

Rögl, F. 1998. Palaeogeographic considerations for Mediterranean and Paratethys Seaways (Oligocene to Miocene). Annalen des Naturhistorischen Museums in Wien, 99A, p. 279-310.

Sadek, H. 1926. The geography and geology of the district between Gebel Ataqa and El Galala El Bahariya (Gulf of Suez). Geological Survey of Egypt, p. 1-120.

Schattner, U., Z. Ben-Avraham, M. Reshef, G. Bar-Am and M. Lazar 2006. Oligocene-Miocene formation of the Haifa basin: Qishon-Sirhan rifting coeval with the Red Sea-Suez rift system. Tectonophysics, v. 419, p. 1-12.

Schlumberger, C. 1990. Note sur le genre Miogypsina. Bulletin de la Société Géologique de France, v. 28, no. 3, p. 327-333.

Seilacher, A. and T. Aigner 1991. Storm deposits at the bed, facies, and basin scale: the geologic perspective. In, G. Einsele, W. Ricken and A. Seilacher (Eds.), Cycles and Events in Stratigraphy. p. 249-267.

Shaaban, F., R. Lutz, R. Littke, C. Bueker and K. Odisho 2006. Source-rock evaluation and basin modelling in NE Egypt (NE Nile Delta and Northern Sinai). Journal of Petroleum Geology, v. 29, no. 2, p. 103-124.

Sharland, P.R., D.M. Archer, D.M. Casey, R.B. Davies, A.P. Hall, A.D. Horbury and M.D. Simmons 2001. Arabian Plate Sequence Stratigraphy. GeoArabia, Special Publication no. 2, 371 p.

Sharland, P.R., D.M. Casey, R.B. Davies, M.D. Simmons and O.E. Sutcliffe 2004. Arabian Plate Sequence Stratigraphy – revisions to SP2. GeoArabia, v. 9, no. 1, p. 199-214.

Shukri, N.M. 1954. On cylindrical structures and coloration of Gebel Ahmar near Cairo, Egypt. Bulletin of the Faculty of Science, Cairo University, v. 32, p. 1-23.

Simons, E.L. 1959. An Anthropoid frontal bone from the Fayum Oligocene of Egypt: The oldest skull fragments of a higher primate. American Museum Novitates, p. 1-16.

Simons, E.L. 1967. The earliest apes. Scientific American, v. 217, p. 28-35.

Simons, E.L. 1972. Primate evolution: An introduction to man's place in nature. Macmillan, p. 1-390.

Slinger, F.C.P. and J.G. Crichton 1959. The geology and development of the Cachsaran field, southwest Iran. 5th World Petroleum Congress, Section I, Paper 18, p. 1-22.

Soliman, I.S. and H.O. Orabi 2000. Oligocene Stratigraphy and Paleoecology of two Mediterranean off-shore wells, in North Sinai, Egypt. Al-Azhar Bulletin of Science, v. 11, no. 1, p. 187-201.

Taberner, C. and D.W.C. Bosence 1985. Ecological succession from corals to coralline algae in Eocene patch reefs, Northern Spain. In, D.F. Toomey and M.H. Nitecki (Eds.), Paleoalgology: Contemporary Research and Applications, p. 226-236.

van Bellen, R.C. 1956. The stratigraphy of the "Main Limestone" of the Kirkuk, Bai Hassan, and Qarah Chauq Dagh structures in North Iraq. Institute of Petroleum Journal, v. 42, p. 233-263.

van Bellen, R.C., H.V. Dunnington, R. Wetzel and D.M. Morton 1959. Iraq, Lexique Stratigraphique Internationale, III, Asie, v. 10a, 333 p.

Vaziri-Moghaddam, H., M. Kimiagari and A. Taheri 2006. Depositional environment and sequence stratigraphy of the Oligo-Miocene Asmari Formation in SW Iran. Facies, v. 52, p. 41-51.

ABOUT THE AUTHORS

Jochen Kuss was awarded a PHD in 1983 by Erlangen University in Germany following studies on Upper Triassic ramp deposits in the northern Calcareous Alps. From 1983 to 1991 he was an Assistant Professor at the Technical University of Berlin and undertook sedimentologic and stratigraphic work in Egypt and Jordan. In 1991 Jochen joined the University of Bremen. His main research interests are field work-based studies of marine Cretaceous to Paleogene successions in North Africa and the Middle East. Methods used include petrography, (micro) biostratigraphy, geochemistry, remote sensing and basin modeling.

kuss@uni-bremen.de

Mohamed A. Boukhary obtained a PhD in 1973 from Ain Shams University. He was a fellow at Marie Curie University in Paris, France, during the academic year 1979–1980, where he worked on the research field of larger foraminifera (Nummulitacea) with Dr. Alphonse Blondeau. Mohamed served as Assistant Professor of Stratigraphy and Micropaleontology at Qatar University from 1981 to 1985 and in 1987 he became a Professor of Micropaleontology. He joined United Arab Emirates University in 1993, and became Chairman of the Geology Department between 1996 and 1998. Mohamed has been Chairman of the Geology Department at Ain Shams University from 2003 to 2007. He has published numerous articles in many international journals.

mboukhary@hotmail.com